Journal of Power Sources 273 (2015) 937–944

Contents lists available at ScienceDirect

Journal of Power Sources

journal homepage: www.elsevier.com/locate/jpowsour

Free volume of mixed cation borosilicate glass sealants elucidated by positron annihilation lifetime spectroscopy and its correlation with glass properties

Prasanta K. Ojha [a, *], Sangram K. Rath [a], Sandeep K. Sharma [b], Kathi Sudarshan [b], Pradeep K. Pujari [b], Tapas K. Chongdar [a], Nitin M. Gokhale [a]

[a] Naval Materials Research Laboratory, Addl. Ambernath, Thane 421506, Maharashtra, India
[b] Radiochemistry Division, Bhabha Atomic Research Centre, Mumbai 400085, India

HIGHLIGHTS

- $Sr_{45-x}L_xA_{10}B_{40}S_5$ glass structure becomes open and rigid on substitution of Sr^{+2} by La^{+3}.
- PALS finds increase in free volume with increasing substitution of Sr^{+2} by La^{+3}.
- Substitution of Sr^{+2} by La^{+3} results in increase in T_g and T_s of glass.
- Thermal stability, CTE and conductivity decrease by substitution of Sr^{+2} by La^{+3}.

ARTICLE INFO

Article history:
Received 22 August 2014
Received in revised form
23 September 2014
Accepted 1 October 2014
Available online 8 October 2014

Keywords:
Mixed cation borosilicate glass sealant
Positron annihilation lifetime spectroscopy (PALS) of glass
Free volume of glass
Molar volume
Packing fraction

ABSTRACT

The role of La^{+3}/Sr^{+2} ratios, which is varied from 0.08 to 5.09, on density, molar volume, packing fraction, free volume, thermal and electrical properties in strontium lanthanum aluminoborosilicate based glass sealants intended for solid oxide fuel cell (SOFC) applications is evaluated. The studies reveal expansion of the glass network evident from increasing molar volume and decreasing packing fraction of glasses with progressive La^{+3} substitutions. The molecular origin of these macroscopic structural features can be accounted for by the free volume parameters measured from positron annihilation lifetime spectroscopy (PALS). The La^{+3} induced expanded glass networks show increased number of subnanoscopic voids with larger sizes, as revealed from the ortho-positronium (o-Ps) lifetime and its intensity. A remarkably direct correspondence between the molar volume and fractional free volume trend is established with progressive La_2O_3 substitution in the glasses. The effect of these structural changes on the glass transition temperature, softening temperature, coefficient of thermal expansion, thermal stability as well as electrical conductivity has been studied.

1. Introduction

Planar solid oxide fuel cell (SOFC) stack requires a high temperature sealant for edge sealing. Thermophysical and thermochemical compatibility and stability in SOFC operational conditions are the major requirements of a material for its suitability as sealant. Borosilicate glasses and glass ceramics with different combinations of modifiers are widely investigated by SOFC researchers as sealants for planar SOFC stacks [1–4]. Our group has also reported several modified aluminoborosilicate glasses suitable for SOFC sealant applications [5–8]. The composition based tailorable properties along with electrical insulating properties are the salient features of these glasses which makes them suitable for SOFC sealant application. Most of the reports on glass sealants address the variation of glass properties with its composition and the correlations including anomalies have been established from glass microstructures probed by various characterization techniques such as X-ray diffraction, scanning electron microscopy, Fourier transformed infrared, Raman and nuclear magnetic resonance spectroscopy [9–15].

The oxide glasses are random networks which are three dimensionally connected by bridging oxygen atoms of network

* Corresponding author. Tel.: +91 251 2623219; fax: +91 251 2623004.
E-mail address: pkojha77@yahoo.co.in (P.K. Ojha).

http://dx.doi.org/10.1016/j.jpowsour.2014.10.005
0378-7753/

forming species. Addition of modifier cations into the glass structure disrupts the network connectivity and their charges are compensated by the surrounding non bridging oxygens (NBO). Additive cations in the glass composition also play a similar role to modifier cations in the glass structure. Extent of network modification depends upon the field strength, F of the cation, expressed as:

$$F = \frac{z_1 z_2 e^2}{r^2} \tag{1.1}$$

where, z_1 and z_2 are the valency of a cation and oxygen respectively, 'e' is the electron charge and 'r' is the distance between cation and oxygen ion [16]. Generally, higher the field strength, higher is the network modification.

Owing to the random structure of glass, a part of the total volume remains unoccupied by atoms, called the free volume. At the fundamental level, free volume is a key parameter that governs the physical properties with compositional feature of glasses. The free volume and its distribution in the glass structure is a composition dependent function. Therefore, variation in free volume in the glass matrix consequent to the structural changes by modifier/additive cations results in variation of glass properties. Ionic substitution is a widely used method for tailoring the properties of ionic oxide glasses. It is thus of fundamental interest to understand the microstructural changes induced by such ionic substitutions. Although the variety of techniques hitherto used has allowed elucidating the residual medium-range structural order of non-crystalline materials, there is still a lack of techniques that are especially sensitive to the nano-sized open volume of materials. Positron annihilation is a sensitive technique used to investigate the size and distribution of sub-nanometre voids of atomic and quasi atomic sizes in polymers [17–19] and metals [20–22]. As regards its application in glasses, to the best of our knowledge, PALS is limited to the micro-structural investigation in topologically disordered chalcogenide glasses [23,24] and free volume anomalies in mixed cation glasses [25,26]. There are also few reports correlating electrical properties of glasses with the free volume of the glass structure [27,28]. However, this technique is equally suitable for different solid-state substances despite their structural hierarchy.

Basically, the glass properties are related to inter-atomic forces as well as the local structure. Therefore, the addition of modifier and additive oxides can introduce change in the local structure as well as energy distribution resulting change in properties of SOFC glass sealant. Common network modifiers used for SOFC glass sealants are alkaline earth oxides such as BaO, SrO, CaO and MgO [29] as they modify glass properties such as glass transition temperature (T_g), glass softening temperature (T_s) and coefficient of thermal expansion (CTE). As nucleating agents, the effect of rare earth metal oxides on T_g and T_s is similar to that of glass network modifiers. La_2O_3 is the most frequently used nucleating agent. Addition of La_2O_3 in the glass composition modifies the viscosity of the glass sealant in SOFC operational condition [29].

In the present work, a series of modified borosilicate glasses with mixed cations (Sr^{+2} and La^{+3}) in the composition designed for SOFC sealant application, are investigated to quantify the free volume through PALS. The molar volume and packing fraction of glass network have been calculated using standard equations. The thermal properties of these glasses such as T_g, T_s, thermal stability ($T_p - T_g$), T_p being the first crystallization temperature and CTE are determined by differential scanning calorimetry (DSC) and dilatometry. Electrical conductivity of the glasses is also measured at 650 °C and all these properties are correlated with the glass structure and the free volume parameters obtained from PALS.

2. Experimental

A series of glasses with nomenclature $Sr_{45-x}L_xA_{10}B_{40}S_5$ ($x = 5, 10 \ldots 40$), where Sr stands for SrO, L for La_2O_3, A for Al_2O_3, B for B_2O_3 and S for SiO_2 and the subscript representing the wt.% of individual oxide component, were prepared using analytical grade reagents $SrCO_3$, La_2O_3, Al_2O_3, H_3BO_3 and SiO_2, procured from Indian sources. The homogenized mixture of a batch composition was melted at 1500 °C using platinum crucible in an electric furnace and the melt was poured into a brass mould to form the glass. After sufficient rigidification on brass mould, the glass melt was transferred to an annealing furnace to eliminate the residual stress created due to rapid cooling. Annealing temperatures of glasses were decided close to their respective T_g. Heating schedule for annealing was fixed at a heating rate of 5 °C min^{-1} upto annealing temperature, holding for 1 h at annealing temperature and cooling to room temperature at a rate of 1 °C min^{-1}.

Phases formed after melt quenching and annealing of batches were evaluated by X-ray Diffraction (XRD) using XPert MPD, PAnalytical instrument, Netherlands. The CuK_α radiation ($\lambda = 1.5418$ Å) from a copper target coupled with Ni filter, was deployed for recording the diffraction pattern of powder samples at room temperature between 20 and 80° (2θ) with 0.005° step size.

Density of the glass samples was measured at room temperature by Archimedes principle in accordance to ASTM C729 with water assuming its density to 1.0 g/cc. The densities of glasses (d_{glass}) were calculated using the following equation:

$$d_{glass} = \frac{M_w}{M_w - M_l} \tag{2.1}$$

where, M_w is the weight of a glass in air and M_l is the suspended weight of the glass immersed in water. A microbalance, SHIMADZU Japan make, was used for this purpose.

The measured glass densities were used to calculate the molar volume (V_m) and packing fraction (C) of the glasses. These parameters were calculated to obtain structural information of the studied glasses as a function of the composition variation. V_m was calculated by using the expression:

$$V_m = \frac{\sum x_i M_i}{\rho} \tag{2.2}$$

where x_i and M_i are the atomic fractions and the atomic weights of Sr, La, Al, B, Si and O respectively and ρ is the measured glass density. The packing fraction, C, was calculated according to the following expressions [30]:

$$C = \frac{V_{ion\ total}}{V_m} \tag{2.3}$$

$$V_{ion\ total} = \sum (N_v V_i f) \tag{2.4}$$

$$V_i = \frac{4}{3}\pi r_i^3 \tag{2.5}$$

where N_v is the Avogadro's number, r_i is the ionic radius (Å) of a cation or an anion having a given coordination number in the glass and f is a conversion factor from $Å^3$ to cm^3. The ionic radii used for the calculations were chosen from those reported by Shannon [31], taking into account the probable coordination of each ion in the glass network, which was determined from related literature [29,32]. In this way, a coordination number 4 was assumed for Si^{+4}, B^{+3} and Al^{+3}, while coordination number of 6 was assumed for Sr^{+2}

and La^{+3} and a coordination number of 6 was assumed for O^{2-} anion in the glass network.

The PALS measurements were performed at room temperature using plastic scintillation detectors coupled in fast–fast coincidence mode. The time dispersion used for acquisition of PALS spectra was 12.5 ps and the time resolution of the spectrometer was 270 ps (full width at half maximum, measured using ^{60}Co). Each specimen consisted of a system of circular discs, of total size 10 mm diameter and 1.2 mm thickness. A ^{22}Na isotope positron source of 2.64 MBq activity sealed in two kapton foils (7 μm thick) was sandwiched between two identical sample discs. More than 1×10^6 counts were acquired in each PALS spectrum. In order to estimate the positron annihilation fraction in kapton films as well as in source material, a reference spectrum of Si single crystal was also acquired.

The T_g and T_p of glass samples were determined using Setsys 16, SETARAM, France. Differential scanning calorimetry (DSC) traces were recorded at the heating rate 5 °C min^{-1} in the temperature range 25–1200 °C. Thermal stability of glasses was calculated as the temperature lag between glass transition and first crystallization temperature, i.e. $(T_p - T_g)$.

Thermal expansion of glass samples was measured using a vertical pushrod type dilatometer of UNITHERM™ MODEL 1161 Dilatometer System, Anter Corporation, USA. All measurements were carried out in atmospheric air. Thermal expansion of glass was measured in temperature range 30–800 °C and at a heating rate of 3 °C min^{-1}. Samples used for these measurements were rod shaped with a length of ≈2.5 cm and diameter ≈0.5 cm. Linear coefficient of thermal expansion (CTE) α was calculated using the following equation:

$$\alpha = \frac{L_1 - L_0}{L_0(T_1 - T_0)} = \frac{\Delta L}{L_0 \Delta T} \quad (2.6)$$

where, L_0 and L_1 are the lengths of the glass specimen at start temperature T_0 under consideration and the end test temperature T_1 respectively. Softening temperature (T_s) of the glasses was determined as point of maximum expansion from their respective expansion plots recorded through dilatometer, following which contraction due to deformation sets in.

Electrical conductivity of the glass samples was measured at 650 °C, using two probe techniques. A glass pellet was sandwiched between two platinum leads, and mounted in a high temperature furnace. Voltage was applied across the sample at the desired temperature and from the measured current flow, resistance was calculated. Conductivity of the sample was calculated from the resistance value considering the structure factor. Impedance Spectroscopy of AUTOLAB, ECO CHEMIE, The Netherlands was used for above measurement.

3. Results and discussion

3.1. Density, molar volume and packing fraction

The different batch compositions used to prepare glasses and the code for each such composition is enlisted in Table 1.

The batch compositions were designed with weight percent (wt.%) of components for ease of calculation. The batch composition was ascribed with a glass code comprising alphabets representing the components and subscript depicting wt.% of the component in the composition. For composition property correlation, mole% of component was calculated using the wt.% and standard molecular weight of the component oxide. Each batch was passed through the melt quenching process as mentioned in the experimental section and after annealing the sample was characterized through XRD for phase analysis. Fig. 1 shows a representative XRD plot of a sample.

Table 1
Batches for glass making with code and composition.

Glass code	Composition (wt.%)				
	SrO	La_2O_3	Al_2O_3	B_2O_3	SiO_2
$Sr_{40}L_5A_{10}B_{40}S_5$	40	5	10	40	5
$Sr_{35}L_{10}A_{10}B_{40}S_5$	35	10	10	40	5
$Sr_{30}L_{15}A_{10}B_{40}S_5$	30	15	10	40	5
$Sr_{25}L_{20}A_{10}B_{40}S_5$	25	20	10	40	5
$Sr_{20}L_{25}A_{10}B_{40}S_5$	20	25	10	40	5
$Sr_{15}L_{30}A_{10}B_{40}S_5$	15	30	10	40	5
$Sr_{10}L_{35}A_{10}B_{40}S_5$	10	35	10	40	5
$Sr_5L_{40}A_{10}B_{40}S_5$	5	40	10	40	5

The plot in Fig. 1 indicates the amorphous phase formed during the melt quench process with no residual crystalline phase either from the precursor oxides or any newly formed crystalline phase during the process. Any such crystalline phase may affect the thermal stability of the glass and hence its thermal properties. The XRD patterns of all investigated compositions after melt quenching and annealing were similar to the presented diffractogram.

Densities of glasses were measured using the Archimedes principle as described in the experimental section and the molar volume of each such glass sample was calculated using Eq. (2.2). Fig. 2 shows the variation of glass density with La^{+3}/Sr^{+2} ratios in the glass composition. The glass density is found to increase with increase in La^{+3}/Sr^{+2} ratios. This may be due to higher atomic weight of La compared to Sr; substituting SrO by La_2O_3 in the glass composition causes an effective increase in mass despite a change in volume with a net result of increase in density of the matrix.

The molar volume (V_m) of the glasses is a calculated entity from the measured density and molar mass of the sample as mentioned in the experimental section. Molar volumes of glasses were calculated and plotted against La^{+3}/Sr^{+2} ratios in the glass composition as shown in Fig. 3.

From Fig. 3, it is observed that incorporation of La_2O_3 systematically increases the molar volume, with no obvious breaks which might indicate a significant change in the structure/composition behaviour of the glasses. This may be due to the higher molar volume of La_2O_3 i.e. 50.05 cc/mol compared to 22.05 cc/mol of SrO [32]. Usually, the density of glasses changes inversely with molar volume. However, in the present case, both the density and molar volume increase with La^{3+} substitution. In order to obtain further structural information with progressive substitution of SrO by La_2O_3, the packing fraction of the glasses was calculated using Eqs.

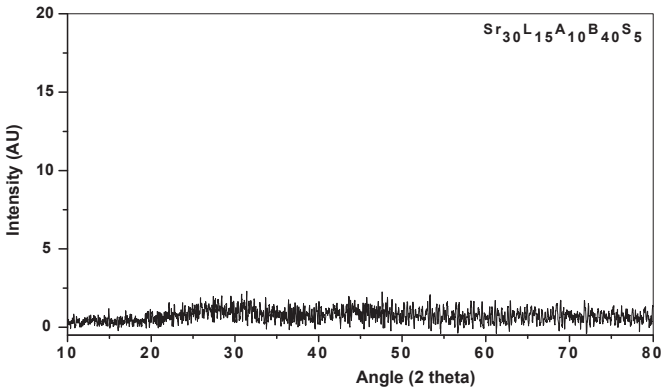

Fig. 1. A representative XRD plot of $Sr_{30}L_{15}A_{10}B_{40}S_5$ glass.

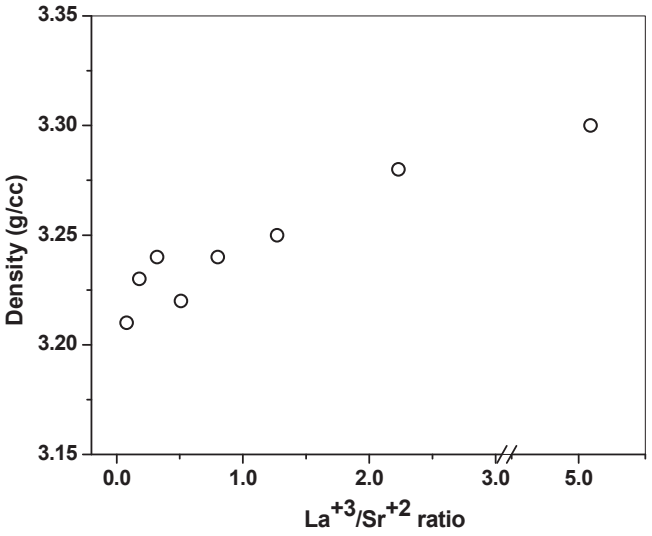

Fig. 2. Variation of glass density with La^{+3}/Sr^{+2} ratios in the glass composition.

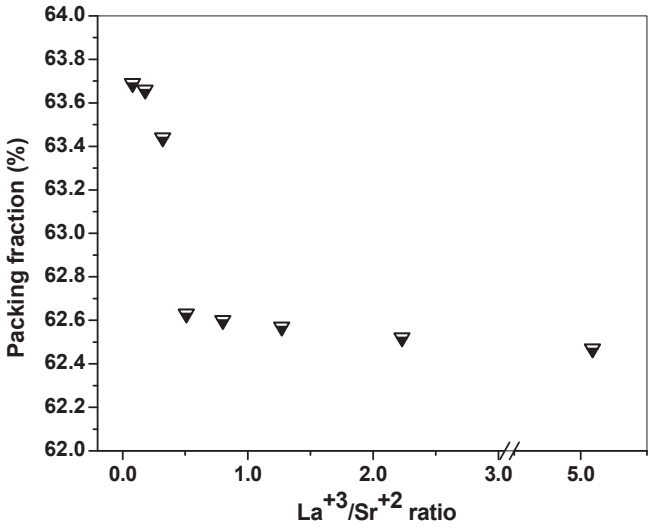

Fig. 4. Packing fraction of glasses vs. La^{+3}/Sr^{+2} ratios in the composition.

(2.3)–(2.5). A plot of packing fraction against La^{+3}/Sr^{+2} ratios in the glass matrix is presented in Fig. 4.

The packing fraction of the glasses shows a decreasing trend with increasing substitution of SrO by La_2O_3; a more pronounced decrease with initial substitutions i.e. La^{+3}/Sr^{+2} ratios below 1, followed by a steady drop. The increasing trend of V_m indicates that an expansion of the glass network occurs due to the partial substitution of SrO by a La_2O_3. This is confirmed by the behaviour of the packing fraction (C), which decreased with increasing La_2O_3 substitution level. The expansion and the concomitant decrease in compactness observed in the glasses, imply an increased distance between the modifying cations upon La_2O_3 substitution. This trend may be attributed to the substitution of lanthanum having larger ionic radius as compared to strontium which is being replaced, in 6-coordination state in the glass network [33]. Angeli et al. [34] have recently shown from NMR studies that addition of lanthanum induces increased disorder in a borosilicate glass, resulting in wider distance and bond angle distributions.

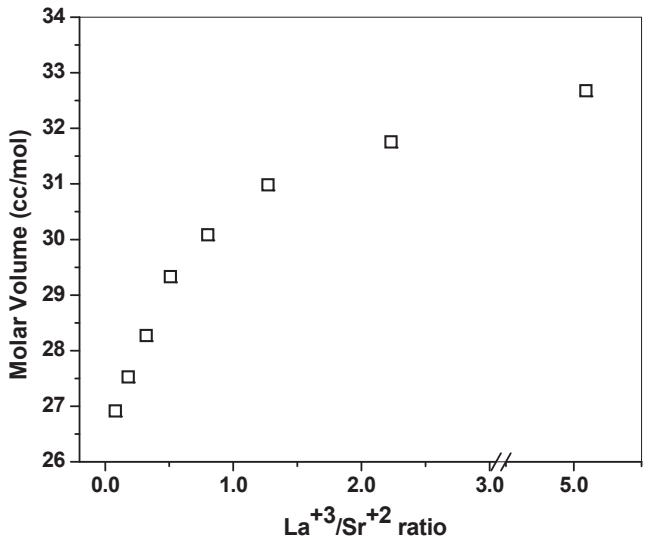

Fig. 3. Plot of molar volume against La^{+3}/Sr^{+2} ratios in the glass composition.

3.2. Free volume analysis from PALS

The positron lifetime spectra were analyzed using the PATFIT computing program with a three-component model [35]. A preliminary analysis of PALS data after correction for positron annihilation in the source and subtracting the background showed the presence of three lifetime components. The first component was observed to vary in the range of 120–160 ps for different samples. In glassy materials, the short-lived component is usually ascribed to para-positronium (p-Ps) annihilation and its lifetime being very short (125 ps in vacuum) is not really affected by the material characteristics. Therefore, in order to reduce the number of fitting parameters, the shortest lifetime τ_1 was fixed at 125 ps for fitting of spectra [36,37].

The intermediate lifetime (τ_2 ~ 0.3 ns) is due to annihilation of free positrons with electrons at vacant sites in oxide materials [37] and hence is of not much informative for the above investigated system. The longest component (τ_3) varies in the range of ~700–800 ps and is ascribed to the ortho-positronium (*o*-Ps) pick-off annihilation in these materials. When, *o*-Ps are confined to cavities their average lifetimes depend on the cavity sizes. The lifetime of *o*-Ps in vacuum is 142 ns [25]. However, in condensed matter, lifetime is shortened to a few ns since the annihilation rate depends on the probability of the overlap of the *o*-Ps wave_function with the wave_functions of the surrounding electrons which is dependent on the cavity size. The intensity of the o-Ps component (I_3) is related to the *o*-Ps formation probability and indicates the concentration of cavities accessible to *o*-Ps.

If R is the radius of the cavity (assuming a sphere) from which the *o*-Ps is annihilating, the *o*-Ps pick-off lifetime is related to the radius of the cavity as per Tao-Eldrup model [38,39].

$$\tau_{o-Ps} = \frac{1}{2}\left[1 - \frac{R}{R+\Delta R} + \frac{1}{2\pi}\sin\left(\frac{2\pi R}{R+\Delta R}\right)\right]^{-1} \quad (3.1)$$

where, $\tau_{o\text{-}Ps}$ is the *o*-Ps pickoff lifetime, ½ pre-factor is the inverse of the spin averaged Ps annihilation lifetime and ΔR is the empirical electron layer thickness which is calibrated to be 0.168 nm for SiO_2 based systems as 1.68 Å. [40]. Accordingly the volume of the void may be calculated from R.

The objective of the present work is to explore the correlation between free volumes and properties of the SOFC sealant

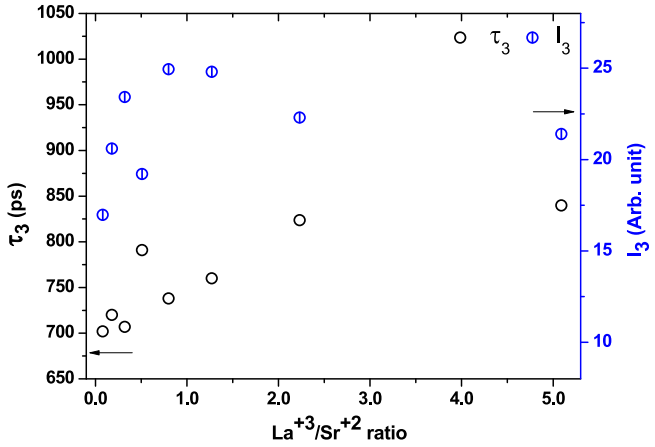

Fig. 5. Variation of τ_3 and I_3 with La^{+3}/Sr^{+2} ratio in the glass compositions.

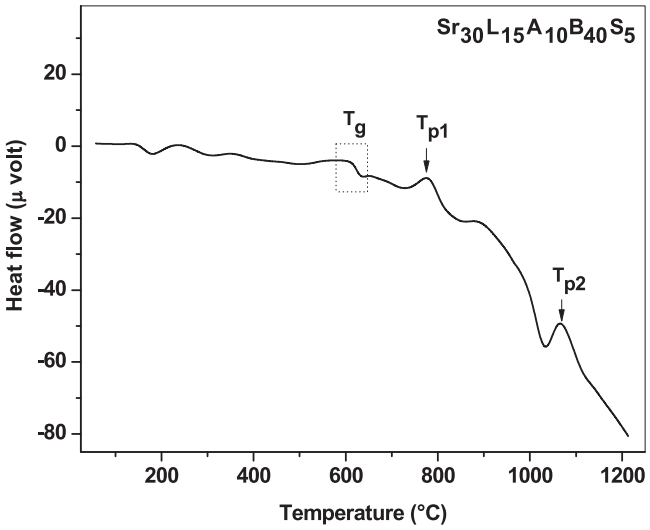

Fig. 7. DSC plot of $Sr_{30}L_{15}A_{10}B_{40}S_5$ glass.

materials. We attribute the longest component τ_3 in the PALS to the pick-off annihilation of *o-Ps* trapped in small intrinsic voids (free volume) present in glass network. Hence, we focus on the variation in τ_3 and I_3 of the glasses with increasing substitution of SrO by La_2O_3. Variation of τ_3 and I_3 with La^{+3}/Sr^{+2} ratios in the glass compositions is presented in Fig. 5. It is noteworthy from Fig. 5, that the value of τ_3 varies from 702.0 ps (5% La_2O_3) to 839.9 ps (40% La_2O_3) and in such a narrow range τ_3 can be considered as linearly proportional to void radius according to Tao-Eldrup model. The pick-off intensity is considered related to density of these voids present in the glass network [37]. The results from lowest and highest concentration La_2O_3 samples also imply that La_2O_3 substitution leads to expansion of the glass network with increased number of voids having relatively bigger size (τ_3 and I_3 increases by 137.9 ps and 4.42% from 5% to 20 % La_2O_3, respectively). It must be noted that the variation in τ_3 and I_3 with progressive La_2O_3 substitution is not systematic in a sense that τ_3 and I_3 do not increase continuously with incorporation of La_2O_3 in the matrix. There are some decreases in τ_3 and I_3 values at certain intermediate compositions. The most probable explanation lies in the mechanism of creation of new voids in the network as a result of substitution of Sr^{2+} by La^{3+}. A mechanism wherein a fraction of new voids would be formed as result of combining of previously existing small size voids into large size void can account for the observed irregularities in variation of o-Ps pick-off annihilation parameters. At this moment we are not able to provide evidence for this mechanism solely on the basis of present data and further investigations are required.

In such a scenario, instead of looking at variation of τ_3 and I_3 separately, a more illuminating approach was found to use the parameter $\tau_3^3 I_3$. In the observed range of τ_3, taking τ_3 proportional to the void radius, the parameter $\tau_3^3 I_3$ can be taken as linearly proportional to fractional free volume present in the glass samples. The plot of $\tau_3^3 I_3$ vs. La^{+3}/Sr^{+2} ratios (Fig. 6), reveals a systematic increase in free volume with increasing La_2O_3 substitution, which exactly replicates the molar volume trend with compositional changes plotted in the same figure. Thus we are able to establish a direct correspondence between the V_m determined from the macroscopic density values and the fractional free volume evaluated from the sub-nanometre size voids. Furthermore, the molecular origin of the expansion of the glass network with La_2O_3 substitution leading to increased V_m and decreased C is also accounted for from the free volume trend.

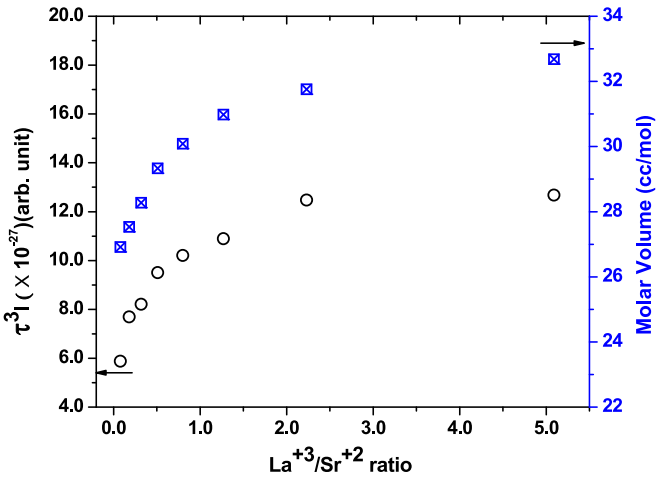

Fig. 6. Free volume and molar volume of glasses against La^{+3}/Sr^{+2} ratios.

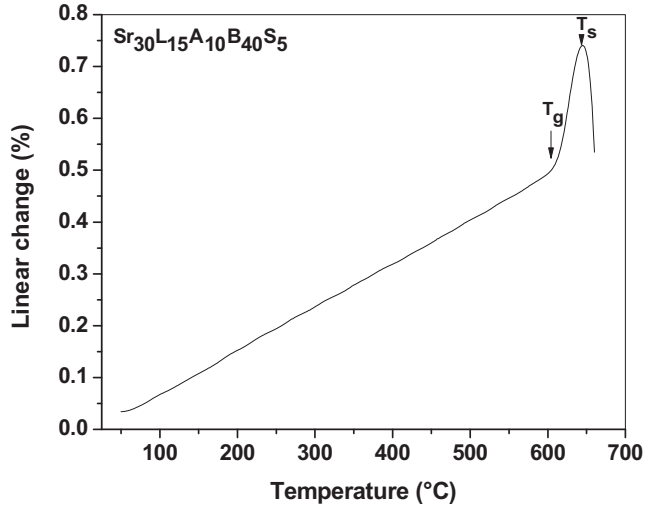

Fig. 8. Expansion plot of $Sr_{30}L_{15}A_{10}B_{40}S_5$ glass obtained from dilatometer.

3.3. Thermal and electrical properties of glasses

Thermal analysis of glass samples was carried out using DSC and dilatometric techniques to determine their characteristic temperatures. Fig. 7 shows a representative thermogram of $Sr_{30}L_{15}A_{10}B_{40}S_5$ glass with glass transition temperature (T_g), and crystallization temperatures (T_{p1} and T_{p2}) marked in the graph. Thermal stability of glass samples was calculated from glass transition temperature (T_g) and 1st crystallization temperature (T_{p1}) by $T_{p1}-T_g$.

The relative expansion of glasses at higher temperatures was recorded through dilatometry and a representative graph is shown in Fig. 8. The dilatometric glass transition (T_g) and softening temperature (T_s) of glasses were noted from the plot as marked in the figure. The CTE of glasses was calculated from the expansion data using the Eq. (2.6). Since the glass transition temperature recorded through dilatometer is for a bulk sample, so for all composition property correlations glass transition temperature (T_g) measured from DSC is presented in subsequent sections.

The glass transition temperature (T_g) is the onset point in the heating cycle when a supercooled liquid converts to a viscoelastic solid, where as the glass softening point (T_s) is the temperature at which the viscous flow changes to plastic flow that means the temperature at which the glass may slump under its own weight. At T_g and T_s, the viscosity corresponds to ~$10^{11.3}$ and ~10^8 Pa s, respectively [32]. For a glass both these characteristic temperatures show a similar trend, however, both depend upon the glass structure and hence on the glass composition. Therefore, to understand the effect of substitution of SrO by La_2O_3 in the investigated series of glasses both T_g and T_s of the glasses are plotted against La^{+3}/Sr^{+2} ratios in the glass composition in Fig. 9.

It can be observed that both glass transition and softening temperature values of the glasses increase with increase in La^{+3} substitutions. Initially, we expected a decrease in T_g of the glasses with La^{+3} substitution based on the observed increased free volume as the bond flexibility increases with creation of free volume. However, the effect of glass modifiers on T_g and T_s of glass also depends on their field strength. Field strength, F, of a modifier cation represents its bonding ability with non bridging oxygen and can be expressed through Eq. (1.1) [16]. Addition of network modifiers into borosilicate glasses increases its T_g and T_s and the extent of increase depends on the cations field strength [16,41]. In the present investigated glass system, La^{+3} as a modifier cation is having higher field strength (0.43), compared to Sr^{+2} (0.27), thereby it modifies the borosilicate network strongly. Therefore, increase in La^{+3}/Sr^{+2} ratios in the glass composition results in an increase in T_g and T_s. Similar observations have been made by Sasmal et al. on the effect of Lanthanum substitution in borosilicate glass systems [42]. The bond strength of La⧹O (244 kJ mol^{-1}) bond is higher than that of Sr⧹O (134 kJ mol^{-1}) or Ca⧹O (134 kJ mol^{-1}) and field strength of La^{+3} (0.52) ion is higher than that of Sr^{+2} (0.32) or Ca^{+2} (0.36) [43,44]. So the addition of La_2O_3 has made the glasses more rigid leading to increase in T_g and T_s. Hence it can be concluded reasonably that substitution of Sr^{+2} by La^{+3} in the glass matrix makes the glass network an open (higher free volume) but rigid (strongly bonded) network evident by the increase in free volume, glass transition and softening temperatures. To estimate the effect of such substitution on the thermal stability of glasses, thermal stability of glasses as calculated from DSC data are plotted against La^{+3}/Sr^{+2} ratios in Fig. 10. Thermal stability of a glass is defined as the resistance to crystallization under the guiding force

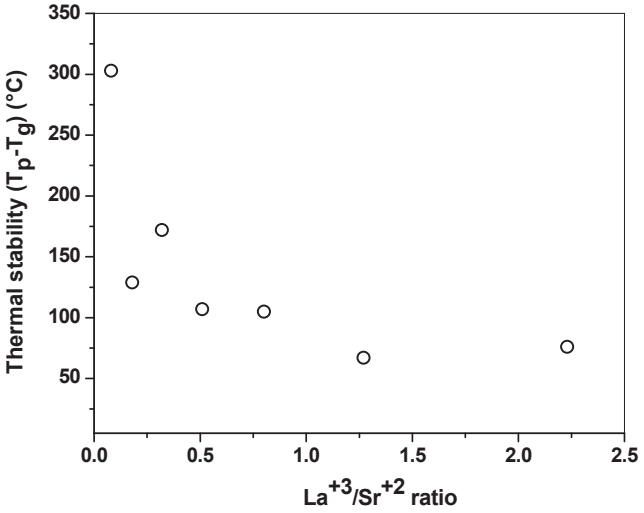

Fig. 10. Thermal stability against La^{+3}/Sr^{+2} ratios in the glass composition.

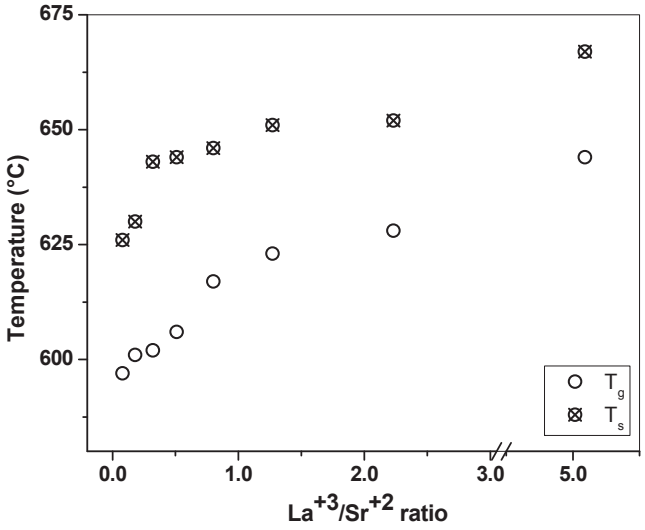

Fig. 9. Variation of T_g and T_s of glasses with La^{+3}/Sr^{+2} ratios in the composition.

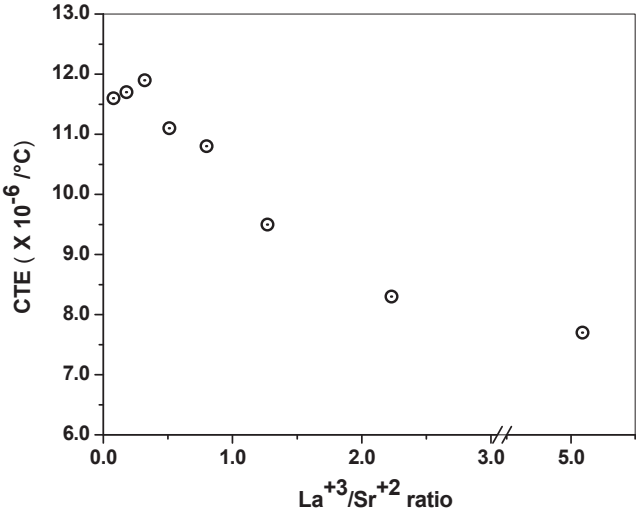

Fig. 11. Coefficient of thermal expansion (CTE) of glasses against La^{+3}/Sr^{+2} ratios.

of thermal energy. This in general depends upon the physical structure of a glass. If the glass structure favours the thermodynamics of crystallization, thermal stability of the glass tends to be low. In the investigated series of glasses, substitution of Sr^{+2} by La^{+3} in the glass matrix increases the free volume of glasses which would favour the crystallization thermodynamics [35,36]. Therefore with increase in La^{+3}/Sr^{+2} ratios from 0.08 to 5.09 in the glass composition the thermal stability decreases from 303 °C to 76 °C.

The degree of expansion with respect to change in temperature is called the material's coefficient of thermal expansion (CTE) and generally CTE of a glass depends on the glass structure symmetry, bond-bending, and molar-free volume. Fig. 11 shows the variation of CTE of glasses with La^{+3}/Sr^{+2} ratios in the glass composition.

The CTE of glasses is found to decrease almost exponentially with increase in Sr^{+2} substitutions by La^{+3}. It is established that modifiers in silicate glasses create non-bridging oxygen species which decrease the average symmetry of the Si–O bonds and thus increase the CTE [21]. On the other hand, CTE decreases if the molar volume and bond-bending of a glass increase [21]. In alkaline earth oxide glasses, CTE decreases with the field strength of the modifier ion [22]. In the present case, La^{+3} has a higher field strength compared to Sr^{+2} and on substitution of Sr^{+2} by La^{+3}, the free volume of the glass increases as mentioned in previous sections. Therefore, the combined effect of higher free volume and higher field strength is presumed to be the reason for decreasing CTE of the glasses with increase in La^{+3}/Sr^{+2} ratios in the glass composition.

Finally, we have investigated the effect of ionic substitution on the electrical conductivity of the glasses. Most oxide glasses including silicates and borosilicates are ionic conductors in which the conductivity is due to the mobility of oxide ions, which in turn depends on the glass composition and structure. The variation of electrical conductivity against La^{+3}/Sr^{+2} ratios in the glass composition is presented in Fig. 12.

From the figure, it is observed that the conductivity decreases significantly with La^{+3} substitutions. The electrical resistivity increases with valence of modifier ions because of the resultant lower ionic mobility [29,32]. A similar phenomena seems to be operative in the present case, with increase in substitution of a divalent Sr^{+2} modifier ion by a trivalent La^{+3} modifier ion, the conductivity decreases due to lower ionic mobility of non bridging oxide ions as also reflected from increased T_g values of the La^{+3} substituted glasses.

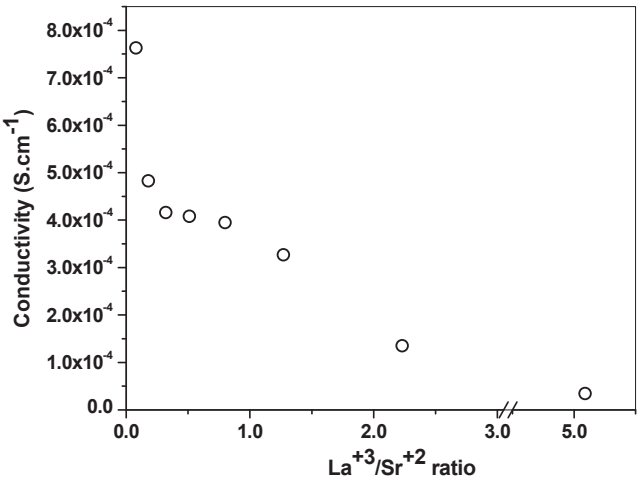

Fig. 12. Electrical conductivity as a function of La^{+3}/Sr^{+2} ratios in glass composition.

4. Conclusion

The glass structure of the presently investigated mixed cation borosilicate glasses, $Sr_{45-x}L_xA_{10}B_{40}S_5$ ($x = 5, 10 \ldots 40$), on substitution of Sr^{+2} by La^{+3} in the glass matrix, becomes an open (higher free volume) but rigid (strongly bonded) network. The network opening was experimentally evident by the increase in free volume measured through *ortho*-positronium probe and was supported by the increase in molar volume calculated from the measured density of the glass matrix and decreased packing fraction. Such a modification in the physical structure of the glass network results in an increase in glass transition and softening temperature, a decrease in thermal stability, coefficient of thermal expansion and electrical conductivity of glasses.

References

[1] J.W. Fergus, J. Power Sources 147 (2005) 46–57.
[2] P.A. Lessing, J. Mater. Sci. 42 (2007) 3465–3476.
[3] S.T. Reis, R.K. Brow, J. Mater. Eng. Perform 15 (2006) 410–414.
[4] V.A.C. Haanappel, V. Shemet, S.M. Gross, T. Koppitz, N.H. Menzler, M. Zahid, W.J. Quadakkers, J. Power Sources 150 (2005) 86–100.
[5] P.K. Ojha, S.K. Rath, T.K. Chongdar, N.M. Gokhale, A.R. Kulkarni, J. Power Sources 196 (2011) 4594–4598.
[6] P.K. Ojha, T.K. Chongdar, N.M. Gokhale, A.R. Kulkarni, Int. J. Hydrogen Energy 36 (2011) 14996–15001.
[7] P.K. Ojha, S.K. Rath, T.K. Chongdar, N.M. Gokhale, A.R. Kulkarni, New J. Glass Ceram. 1 (2011) 21–27.
[8] P.K. Ojha, T.K. Chongdar, N.M. Gokhale, A.R. Kulkarni, J. Power Sources 221 (2013) 28–34.
[9] M.K. Mahapatra, K. Lu, W.T. Reynolds Jr., Thermophysical properties and devitrification of SrO-La_2O_3-Al_2O_3-B_2O_3-SiO_2 based glass sealant for solid oxide fuel/electrolyzer cells, J. Power Sources 179 (2008) 106–112.
[10] V. Kumar, A. Arora, O.P. Pandey, K. Singh, Int. J. Hydrogen Energy 33 (2008) 434–438.
[11] S. Sen, P. Yu, V.P. Klyuev, B.Z. Pevzner, J. Non-cryst. Solids 354 (2008) 4005–4011.
[12] B. Tiwari, A. Dixit, G.P. Kothiyal, Int. J. Hydogen Energy 36 (2011) 15002–15008.
[13] S. Ghosh, P. Kundu, A.D. Sharma, R.N. Basu, H.S. Maiti, J. Eur. Ceram. Soc. 28 (2008) 69–76.
[14] P.H. Gaskell, Nucl. Instrum. Methods 199 (1982) 45–60.
[15] M.K. Mahapatra, K. Lu, J. Power Sources 185 (2008) 993–1000.
[16] H. Scholze, Glass Nature, Structure and Properties, Springer Verlag, New York, 1991.
[17] P.N. Patil, S.K. Rath, S.K. Sharma, K. Sudarshan, P. Maheshwari, M. Patri, S. Praveen, P. Khandelwal, P.K. Pujari, Soft Matter 9 (2013) 3589–3599.
[18] N. Patil, K. Sudarshan, S.K. Sharma, S.K. Rath, M. Patri, P.K. Pujari, Chem. Phys. Chem. 13 (2012) 3916–3922.
[19] K. Sudarshan, S.K. Rath, M. Patri, A. Sachdeva, P.K. Pujari, Polymer 48 (2007) 6434–6438.
[20] R.S. Vallery, M. Liu, D.W. Gidley, M.E. Launey, J.J. Kruzic, Appl. Phys. Lett. 91 (2007) 261908.
[21] K.M. Flores, E. Sherer, A. Bharathula, H. Chen, Y.C. Jean, Acta Mater. 55 (2007) 3403–3411.
[22] A. Ishii, F. Hori, A. Iwase, Y. Fukumoto, Y. Yokoyama, T.J. Konno, Mater. Trans. 49 (9) (2008) 1975–1978.
[23] O. Shpotyuk, A. Kovalskiy, J. Filipecki, T. Kavetskyy, Phys. Chem. Glas. Eur. J. Glass Sci. Technol. B 47 (2) (2006) 131–135.
[24] O.I. Shpotyuk, J. Filipecki, V.O. Balitska, J. Optoelctr. Adv. Mater. 10 (2008) 3193–3197.
[25] M.D. Ingram, S.J. Pas, C. Cramer, Y. Gao, A.J. Hill, Phys. Chem. Chem. Phys. 7 (2005) 1620–1623.
[26] M. Reben, E. Goli, J. Filipecki, M. Sitarz, K. Kotynia, P. Jeleń, I. Grelowska, Spectrochimica Acta Part A: Mol. Biomol. Spectrosc. 129 (2014) 643–648.
[27] E. Golis, J. Filipeck, M. Reben, J. Wasylak, Chem. Met. Alloys 4 (2011) 18–21.
[28] M.L.F. Nascimento, Braz. J. Phys. 37 (2A) (2007) 429–434.
[29] M.K. Mahapatra, K. Lu, Mater. Sci. Eng. R 67 (2010) 65–85.
[30] A.K. Varshneya, Fundamentals of Inorganic Glasses, Academic Press, San Diego, CA, USA, 1994.
[31] R.D. Shannon, Acta Cryst. A32 (1976) 751–767.
[32] J.E. Shelby, Introduction to Glass Science and Technology, second ed., The Royal society of Chemistry, Cambridge, UK, 2005.
[33] S. Ounnukad, Solid State Commun. 138 (2006) 472–475.
[34] F. Angeli, T. Charpentier, E. Molières, A. Soleilhavoup, P. Jollivet, S. Gin, J. Non-Cryst. Solids 376 (2013) 189–198.
[35] P. Kirkgraad, N.J. Pedersen, M. Eldrup, PATFIT, RISO National Laboratory, Denmark, 1998.
[36] K. Inoue, H. Kataoka, Y. Nagai, M. Hasegawa, Y. Kobayashi, J. Appl. Phys. 115 (2014) 204903.

[37] M. Zanatta, G. Baldi, R.S. Brusa, W. Egger, A. Fontana, E. Gilioli, S. Mariazzi, G. Monaco, L. Ravelli, F. Sacchetti, Phys. Rev. Lett. 112 (2014) 045501.
[38] S.J. Tao, J. Chem. Phys. 56 (1972) 5499.
[39] M. Eldrup, D. Lightbody, N.J. Sherwood, Chem. Phys. 63 (1981) 51–58.
[40] D.W. Gidley, W.E. Frieze, T.L. Dull, A.F. Yee, E.T. Ryan, H.M. Ho, Phys. Rev. B 60 (1999) R5157.
[41] M.B. Volf, Chemical Approach to Glass, Glass Sci Tech, vol. 7, Elsevier, New York, 1984.
[42] N. Sasmal, M. Garai, A.R. Molla, A. Tarafder, S.P. Singh, B. Karmaka, J. Non-Cryst. Sol. 387 (2014) 62–67.
[43] Y.-S. Chou, J.W. Stevenson, P. Singh, J. Electrochem. Soc. 154 (7) (2007) B644–B651.
[44] A. Goel, D.U. Tulyaganov, V.V. Kharton, A.A. Yaremchenko, J.M.F. Ferreira, Act. Mater. 56 (2008) 3065–3076.

Glossary

SOFC: solid oxide fuel cell
PALS: positron annihilation lifetime spectroscopy
NBO: non-bridging oxygens
XRD: X-ray diffraction
DSC: differential scanning calorimetry
CTE: coefficient of thermal expansion